View metadata, citation and similar papers at core.ac.uk

brought to you by CORE

東北大学機関リポジトリ
TOUR
Tohoku University Repository

Growth kinetics and thermal stability of a self-formed barrier layer at Cu-Mn/SiO2 interface

著者	小池　淳一
journal or publication title	Journal of applied physics
volume	102
number	4
page range	043527-1-043527-7
year	2007
URL	http://hdl.handle.net/10097/34908

Growth kinetics and thermal stability of a self-formed barrier layer at Cu-Mn/SiO_2 interface

J. Koike,[a] M. Haneda, and J. Iijima
Department of Materials Science, Tohoku University, Sendai 980-8579, Japan

Y. Otsuka and H. Sako
Toray Research Center Inc., Otsu, Shiga 520-8567, Japan

K. Neishi
Department of Materials Science, Tohoku University, Sendai 980-8579, Japan

(Received 5 June 2007; accepted 12 July 2007; published online 29 August 2007)

A thin diffusion barrier was self-formed by annealing at an interface between a Cu-Mn alloy film and a SiO_2 substrate. The growth of the barrier layer followed a logarithmic rate law, which represents field-enhanced growth mechanism in the early stage and self-limiting growth behavior in the late stage. The barrier layer was stable at 450 °C for 100 h and at 600 °C for 10 h. The interface diffusivity was estimated from the morphology change of the barrier layer at 600 °C and was found to be smaller than the grain-boundary diffusivity of bulk Cu. © *2007 American Institute of Physics*.
[DOI: 10.1063/1.2773699]

I. INTRODUCTION

Large-scale integrated (LSI) devices have an interconnect structure made with conducting metallic materials and insulating dielectric materials. As the feature size of the LSI devices decreases to submicrometer scale, device performance becomes limited mainly by the interconnect delay that is proportional to the product of interconnect resistivity and capacitance. In order to decrease the interconnect delay, the combination of Cu and various low-*k* materials has been considered for advanced LSI devices. Incidentally, Cu interdiffuses easily with dielectric materials, such as SiO_2 and its low-*k* derivative of SiOC. In order to prevent interdiffusion, Ta and TaN are sputter-deposited as barrier layers at an interface between Cu and the dielectric layer.[1] Since the resistivity of the barrier layers is more than an order of magnitude larger than that of Cu, the presence of the barrier layer increases the effective resistivity of the interconnect lines and sacrifices device performance. Therefore, the thickness of the barrier layer should be reduced to a minimum possible value. For instance, the desired barrier thickness is 5.2, 3.3, and 2.4 nm, respectively, for the technology node of 65, 45, and 32 nm for intermediate level interconnects.[2]

Atom layer deposition (ALD) has been considered as a promising method to form a thin conformal barrier layer of the desired thickness. However, intake of precursor-born impurities into Cu and associated reliability problems have remained major concerns for the ALD method.[3] Alternatively, a barrier-less process or a self-forming barrier process has been proposed. In this case, Cu is alloyed with a strong oxide former, such as Mg and Al, and the alloy film is deposited directly on a dielectric layer without any conventional barrier layer.[4,5] During heat treatment, the alloying element was supposed to migrate to the interface and to react with the dielectric layer to form an oxide of the alloying element. This interface oxide layer was expected to act as a diffusion barrier layer. However, two major problems had prevented this method from being put into practice. In the first, oxide formation leads to the reduction of the SiO_2 dielectric layer, which makes Si atoms migrate to the Cu interconnect.[6] In the second, the alloying element that is left out from the oxidation reaction tends to remain in the Cu interconnect.[7] Both cases lead to a notable increase in resistivity.

Recently, we reported Cu-Mn alloy as a new material for the self-forming barrier process.[8] The reaction layer formed between the alloy film and SiO_2 was only 3–4 nm in thickness after annealing at 450 °C for 30 min. Residual Mn after annealing could be removed from the alloy film to form a surface oxide layer because of a large activity coefficient of Mn in Cu. This led to a drastic decrease of film resistivity. No interdiffusion was detected between the film and SiO_2. We also found that the Mn concentration is an important factor to control the barrier thickness.[9] This process was applied to a dual damascene interconnect structure with excellent characteristics and reliability. Usui *et al.* reported the self-formation of a barrier layer with a uniform thickness of approximately 2 nm at trench and via interfaces with SiO_2 dielectric.[10] More than 50% reduction in via resistance was obtained in comparison with a conventional Ta barrier layer. No stress-migration failure was observed after annealing at 225 °C for 1600 h. No electromigration failure was observed after 1000 h testing at 325 °C at 1 MA/cm^2 when electron flow was from a lower level interconnect through a via to an upper level interconnect.

In this article, we investigated the growth kinetics and thermal stability of the self-formed barrier layer up to 600 °C. The charged states of Mn and concentration profile were also investigated across the barrier layer with electron energy loss spectroscopy attached to a transmission electron microscope. The growth kinetics between 250 °C and 450 °C and its physical origin were discussed based on the

[a]Corresponding author; FAX +81-22-795-7360; electronic mail: koikej@material.tohoku.ac.jp

 © 2007 American Institute of Physics

Downloaded 11 Jul 2008 to 130.34.135.158. Redistribution subject to AIP license or copyright; see http://jap.aip.org/jap/copyright.jsp

charged state of Mn and associated formation of electric field across the barrier layer. The change in the barrier morphology at 600 °C was used to estimate the interface diffusivity.

II. EXPERIMENTAL PROCEDURE

Alloy films of Cu-10 at. %Mn were deposited to a thickness of 150 nm at room temperature by cosputtering of pure metal targets of Cu(99.9999%) and Mn(99.98%), using a rf magnetron sputtering machine. Substrates were TEOS-SiO_2 of 100 nm in thickness formed by plasma chemical vapor deposition (CVD) on single-crystal Si wafers. The distance between the targets and the substrate was 20 cm, which enabled the films to be formed with spatial uniformity in both composition and thickness.

In this work, three-types of experiments were performed. In the first, characteristic features of a self-formed barrier layer were studied after heat treatment at 450 °C for 30 min in Ar+3 vol % H_2 atmosphere. Transmission electron microscopy (TEM) and electron energy loss spectroscopy (EELS) were used to investigate the microstructure, composition profile, and oxidation state of the annealed sample. Cross-section samples were prepared with a focused ion beam (FIB) microscope. Upon composition analysis, an incident electron beam was focused to a nominal diameter of 0.2 nm and was step-scanned across the sample cross section at 0.2 nm step. At each scanned step, EELS spectra of Cu, Mn, Si, and O were collected and the composition was analyzed. In the second, the growth kinetics of the barrier layer was observed with TEM. In this case, special care was taken to eliminate a secondary effect on the growth kinetics. As shown later, Mn atoms diffuse not only to the interface to form the barrier layer but also to the film surface to form an oxide layer. The outdiffusion of Mn atoms to the film surface would decrease the Mn concentration in the film and eventually dry out the Mn supply to form the barrier layer. In order to prevent this undesirable effect, the alloy film was covered with an additional layer of Ta having a thickness of 50 nm and heat treated in vacuum of 1×10^{-7} Pa. Depth profiling with x-ray photoelectron spectroscopy (XPS) of an annealed sample at 450 °C for 100 h indicated no Mn segregation at the Ta/Cu-Mn interface. EDS analysis of the same sample also indicated a Mn concentration of 6.1 to 6.7 at. % remaining in the film. In the third, thermal stability of the barrier layer was examined at 450 °C and 600 °C up to 100 h in the same vacuum atmosphere. Samples used in this experiment had the Ta top layer to prevent Mn outdiffusion to the film surface. Possible variations of the microstructure and composition profile were investigated with TEM and x-ray energy dispersive spectroscopy (EDS).

III. RESULTS

Figure 1 shows a cross-sectional TEM image after annealing at 450 °C for 30 min. Thin continuous layers are observed on the Cu-Mn film surface and at the Cu-Mn/SiO_2 interface. Figure 2 shows the composition profile analyzed along the arrow in Fig. 1. It is found that Mn and O are segregated at the film surface and at the interface where the thin continuous layers were observed in Fig. 1. Only Cu is detected within the film, and Mn is depleted from the film interior. No interdiffusion is observed between the original Cu-Mn layer and the SiO_2 layer. The absence of interdiffusion indicates that the interface oxide layer acts as a diffusion barrier.

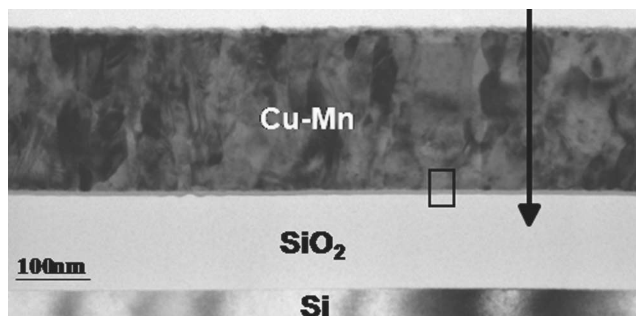

FIG. 1. Cross-sectional TEM image after annealing at 450 °C for 30 min.

Detailed characteristics of the barrier layer are shown in Fig. 3. A high-resolution image in (a), taken from the squared area in Fig. 1, shows that the barrier layer has an amorphous structure. EELS spectra were taken from the six numbered regions and the results are shown in (b) and (c). Careful inspection of Figs. 3(b) and 3(c) indicates that silicon is present in the regions 4–6. A weak Si peak may be present in 3. Oxygen is present in regions 3–6. Manganese is present in regions 2–5. Copper is present in regions 1–3. Therefore, region 1 is pure Cu; region 2 is Cu-Mn; region 3 is Cu-Mn-O; regions 4 and 5 are Mn-Si-O; and region 6 is Si-O. A fine structure of Mn-L edge is shown in Fig. 4 for the selected regions of 2 (Cu-Mn), 4 (Mn-Si-O in the middle of the barrier layer), and 5 (Mn-Si-O at the interface of the barrier layer with SiO_2). Chemical shift of the Mn-*L*3 edge can be seen clearly and the magnitude of the shift depends on the regions. The Mn-*L*3 peak in region 2 (Cu-Mn) appears at the same energy loss of 643 eV as those in region 4 (Mn-Si-O in the middle of the barrier). It should be noted that this value is larger than the expected value of 640 eV for metallic Mn.[11,12] Meanwhile, the Mn-*L*3 peak in region 5 (Mn-Si-O at the interface of the barrier layer with SiO_2) appears at even higher energy loss of 644 eV than the other two peaks. Generally, chemical shift increases with increasing oxidation state. These results suggest that unreacted Mn atoms are segregated near the interface of the barrier layer and present as the Cu-Mn alloy layer. The electronic state of the segregated

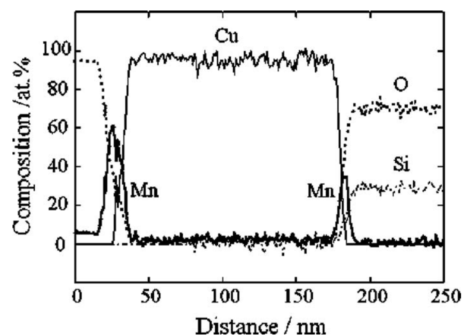

FIG. 2. Composition profile of Cu-Mn/SiO_2 after annealing at 450 °C for 30 min.

Downloaded 11 Jul 2008 to 130.34.135.158. Redistribution subject to AIP license or copyright; see http://jap.aip.org/jap/copyright.jsp

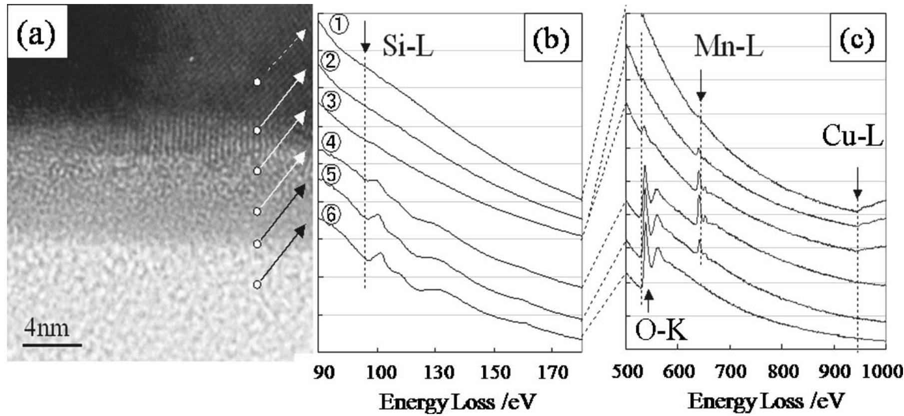

FIG. 3. EELS analysis of the barrier layer formed after annealing at 450 °C for 30 min. (a) High-esolution TEM image; (b) and (c) EELS spectra of the numbered region in (a).

Mn is similar to that of Mn in the barrier layer. Namely, electrons are removed from the Mn atoms in region 2. In contrast, the oxidation state of Mn in region 5 is larger than that in region 3. The difference in the electronic state of Mn may form electric field across the barrier layer and may influence the growth kinetics of the barrier layer. This will be discussed later in detail.

The growth kinetics of the barrier layer was investigated by measuring the thickness of the barrier layer using TEM after annealing at various temperatures. The results are shown in Fig. 5. The data points in the figure are average values measured at ten different locations for each sample. The size of the data points approximately corresponds to measurement error. At all temperatures, the barrier layer grows rapidly in the early stage and grows slowly in the late stage. The maximum thickness of the barrier layer is approximately 4 nm at 250 °C and 350 °C and 7 nm at 450 °C. It should be noted that the slow growth rate in the late stage is not due to the depletion of Mn. The Ta top layer and vacuum annealing can prevent the outdiffusion of Mn to the film surface and keep the concentration of remaining Mn in the film at 6.1 to 6.7 at % even after annealing at 450 °C for 100 h. According to the International Technology Roadmap of Semiconductors (ITRS), the barrier thickness should be less than 5 nm for the technology node of 45 nm and beyond.[2] Figure 4 clearly indicates that the barrier layer formed at 250 °C and 350 °C can satisfy the ITRS requirement independent of annealing time. Annealing at 450 °C up to 2 h also satisfies the requirement.

Thermal stability of the barrier layer was investigated with TEM and EDS. Figure 6 shows a TEM image of an annealed sample at 450 °C for 100 h in (a) and an EDS spectrum from the SiO_2 layer in (b). A continuous barrier layer of 6.9 nm in thickness is observed at the interface. The EDS spectrum from the SiO_2 layer shows no interdiffusion of Cu or Mn, indicating an excellent thermal stability at 450 °C. The results of annealed samples at 600 °C are in a striking contrast as shown in Fig. 7. Though not shown here, a TEM image after 1 h shows virtually the same image as in Fig. 6(a), having a barrier thickness of 7.2 nm. Striking differences are observed after longer annealing. Figures 7(a) and 7(c) show TEM images of annealed samples at 600 °C for 10 and 100 h, respectively. The corresponding EDS spectra are shown in Figs. 7(b) and 7(d). As can be seen in Fig. 7(a), the barrier layer changes its shape at Cu grain boundaries, most likely to establish energy equilibrium at triple points. The interface with the SiO_2 layer is completely flat. Notice that, at the area where an extremely thin barrier layer is observed on the right side, the interfaces formed with Cu, the barrier layer, and the SiO_2 layer are nearly parallel, maintaining the presence of the thin barrier layer. This suggests that these interfaces have very small energy and are very stable. The EDS spectrum in Fig. 7(b) shows no interdiffusion of Cu and Mn into the SiO_2 layer. Figure 7(c) shows the dissociated barrier layer after 100 h. The barrier layer can be seen only at some triple points with Cu grain boundaries. No continuous barrier layer is seen at the interface. The SiO_2 layer shows a darker contrast. The EDS spectrum taken from a region of the dark contrast indicates the presence of Cu in the SiO_2 layer, as shown in Fig. 7(d).

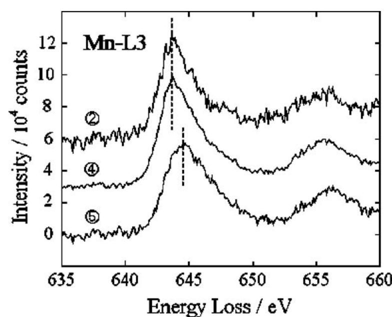

FIG. 4. Fine structure of EELS spectra of Mn-*L* edge on regions 2, 4, and 5.

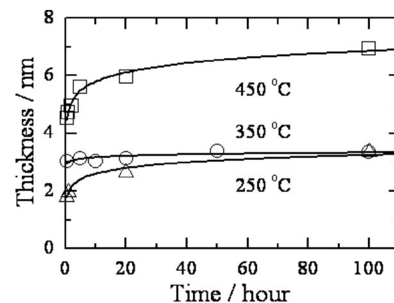

FIG. 5. Thickness variation of the barrier layer at 250 °C, 350 °C, and 450 °C as a function of annealing time.

Downloaded 11 Jul 2008 to 130.34.135.158. Redistribution subject to AIP license or copyright; see http://jap.aip.org/jap/copyright.jsp

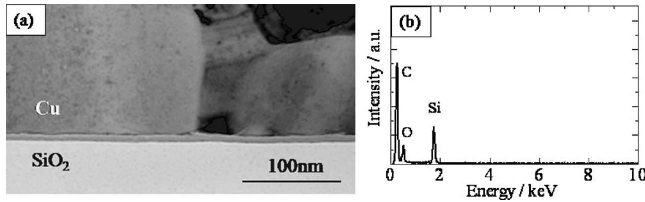

FIG. 6. (a) Cross-sectional TEM image after annealing at 450 °C for 100 h. (b) EDS spectrum taken from the SiO_2 layer.

IV. DISCUSSION

A. Growth kinetics of the self-formed barrier layer

Growth of an oxide layer at high temperatures is rate-controlled by atomic diffusion through the oxide and is known to follow a parabolic rate law.[13] At low temperatures, thermal activation is not sufficient for atomic diffusion and the parabolic rate law breaks down. Instead, a logarithmic rate law was proposed for the low-temperature oxidation.[14] The low-temperature oxidation is based on the assumption of electron or hole tunneling through an initially thin oxide of less than approximately 10 nm in thickness. Under this assumption, potential drop occurs across the oxide by the difference between the work function of metal and the chemical affinity of oxygen. The resulting electric field across the oxide can serve as a driving force for ionic transport, which is considered to be a rate-controlling process of the oxide growth. According to the logarithmic rate law, the oxide thickness increases linearly with a logarithm of annealing time as[14,15]

$$X = A \log(t+1), \tag{1}$$

with the rate constant given by

$$A = \exp\left(\frac{qa\Delta\Phi}{2XkT}\right), \tag{2}$$

where q is the electronic charge of transport ions, a is the distance between moving interstitials, $\Delta\Phi$ is the potential drop across the oxide, and X is the oxide thickness. The parameter, $\Delta\Phi/X$, corresponds to the field strength across the oxide. Though this model was proposed for surface oxidation of metals with chemisorbed oxygen in an oxygen-containing ambient, we adopt these models for a solid-state oxidation, that is, the growth kinetics of the self-formed barrier layer. We consider that this assumption is valid as far as the enhanced ionic diffusion across the oxide is a rate-controlling process.

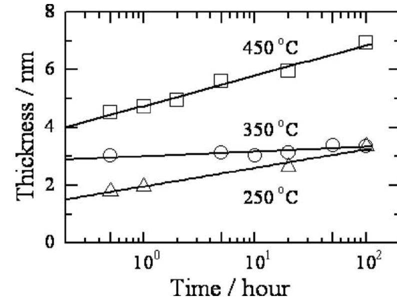

FIG. 8. Thickness variation of the barrier layer plotted as a function of the logarithm of annealing time.

As shown in Fig. 8, the logarithmic plot is found to fit best to the experimental results of the barrier growth at all three temperatures. This indicates that the growth of the barrier layer occurs by the field-enhanced ionic transport. Ionic transport in oxides is generally known to depend on bond strength and local structural ordering.[16] Weakly bonded oxides have a compact and dense structure. In this case, small cations tend to be major transporting ions. Meanwhile, SiO_2 is categorized as a strongly bonded oxide that has random open networks with a high degree of short-range order. In this case, larger anions tend to diffuse through an open network structure. Therefore, we consider that Mn is a dominant diffusing ion within SiO_2. Once Mn ions diffuse into SiO_2, the barrier layer is formed and its growth is rate-controlled by Mn diffusion through the barrier layer.

Keeping this in mind, we now discuss the presence of the electric field across the barrier layer, based on the EELS fine structure of Mn-*L*3 edge shown in Fig. 4. The EELS fine structure revealed that the position of the Mn-*L*3 edge was 643 eV in the Cu-Mn layer adjacent to the oxide interface, 643 eV in the middle of the barrier layer, and 644 eV in the barrier layer adjacent to the SiO_2 interface. The Mn-*L*3 edge of various Mn oxides is known to appear at 640.2 eV for MnO, 642.1 eV for Mn_3O_4, 643.0 eV for Mn_2O_3, and 644.4 eV for MnO_2.[11,12] Comparison of these values suggests that the charged state of Mn in the middle of the barrier layer is close to Mn^{3+}. This result suggests that Mn_2O_3 is a major component in the middle of the barrier layer together with a complex mixture of Cu toward the alloy layer and of Si toward the SiO_2 layer. However, the broad peak shape prevents us from clearly determining the exact charged states of Mn in the barrier layer.

Rather striking results are found in the charged states of Mn in region 2 of Cu-Mn alloy and in region 5 of the barrier layer adjacent to the SiO_2 layer. In region 2, Mn is supposedly in solid solution with Cu and the *L*3 edge of metallic Mn would appear at 640 eV. But, the *L*3 edge appears at 643 eV, indicating the presence of trivalent Mn with its electrons stripped and tunneled through the thin barrier layer. On the other side of the barrier layer, further chemical shift is observed. The *L*3 edge is found at 644 eV, suggesting the pres-

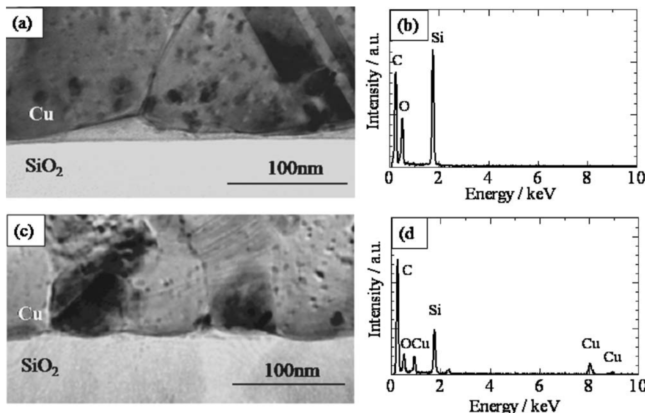

FIG. 7. Cross-sectional TEM images and EDS spectra from the SiO_2 layer after annealing at 600 °C. (a), (b) annealed for 10 h; (c, d) annealed for 100 h.

Downloaded 11 Jul 2008 to 130.34.135.158. Redistribution subject to AIP license or copyright; see http://jap.aip.org/jap/copyright.jsp

ence of Mn^{4+} that may be necessary to compensate the excess electrons originated from the Mn atoms in the Cu-Mn layer. This tunneling process would form electric field across the barrier layer and enhance the diffusion of Mn ions, yielding the logarithmic growth rate of the barrier layer.

B. Temperature dependence of the growth rate

Figure 8 also shows a peculiar temperature dependence of the growth kinetics. With decreasing annealing temperature from 450 °C to 350 °C, the growth rate decreases. Then, with further decreasing temperature to 250 °C, the growth rate increases. It is not clear why the inverse temperature dependence is observed between 250 °C and 350 °C. In this respect, Nakatani *et al.* reported interesting results in trilayer samples of Mn/Si-O/Si.[17] They measured magnetic property before and after annealing at elevated temperatures up to 527 °C in vacuum of 1.3×10^{-4} Pa. Saturation magnetization measured at room temperature indicated ferromagnetism for the annealed samples above 300 °C but not below 250 °C. They suggested that an unknown compound of Mn-Si-O having a Curie temperature of 67 °C is responsible for the ferromagnetic property. Their results also suggest that the structure and composition of the reaction product are different between the samples annealed below 250 °C and above 300 °C. If the same reaction occurs for the self-formed barrier in the present work, it is reasonable to observe the peculiar growth rate at 250 °C in comparison with the rate at 350 °C and 450 °C because of possible difference in ionic diffusivity. Furthermore, Avouris *et al.* pointed out the influence of growth stress on the growth rate.[18] They used AFM to induce electric field and investigated the field dependence on the growth kinetics of oxide on Si (100) surface in air. They observed a linear relationship between the oxide growth rate and the oxide thickness. Since the Cabrera-Mott theory alone would predict nonlinear relation according to the rate constant given in Eq. (2), an additional stress-related term was added to explain the discrepancy. As a result, they concluded that the oxide growth is self-limited not only by decreasing electric field with thickness but also by increasing growth stress. In the present work, if the barrier structure is different below 250 °C and above 300 °C, the growth stress is likely to depend on the barrier structure, giving rise to the difference in the growth rate.

C. Morphology change of the barrier layer at 600 °C

During annealing at 600 °C, the interface between the barrier and SiO_2 remains flat up to 10 h, showing a stable morphology. In contrast, the interface between the barrier and Cu changes its shape probably because of energy balance at triple points formed by the barrier/Cu interfaces and the Cu grain boundaries. This is similar to the formation of grain-boundary grooves on Cu surface; analogous equations can be used by replacing surface energy with interface energy in the following discussion. As shown in Fig. 9, the tangential angle of the interface with respect to the Cu grain boundary, θ, is dependent on the interface energy, γ_{int}, and grain-boundary energy, γ_{gb}, and is given by

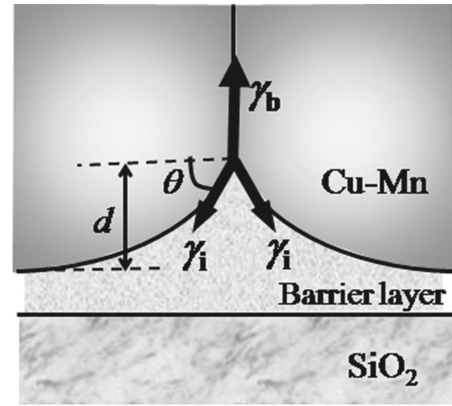

FIG. 9. Schematic figure of the groove formation.

$$\gamma_{gb} = 2\gamma_{int}\sin\theta. \tag{3}$$

Using this equation, we can estimate the interface energy. The tangential angle was measured from ten different triple points in cross-sectional TEM images. An average value was approximately 45°. The energy of general grain boundaries of Cu is 0.625 J/m^2. Then, the interface energy is calculated to be 0.442 J/m^2, approximately 70% of the grain boundary energy.

Borisov *et al.* proposed a theory to derive interface diffusivity from interface energy and volume diffusivity.[19] The theory is based on the approximation that the activation energy of interface diffusion is smaller by the magnitude of the interface energy than that of volume diffusion. Based on this theory, Gupta proposed the following relation between the interface diffusivity, D_{int}, volume diffusivity, D_v, and interface energy:[20]

$$\gamma_{int} = \frac{1}{2}RT\ln\left(\frac{D_{int}}{D_v}\right). \tag{4}$$

This relation holds for general grain boundaries by replacing γ_{int} with γ_{gb}. When the interface energy is equal to $1/n$ of the grain boundary energy, the interface diffusivity can be calculated by simple derivation of Eq. (4) to the following form:

$$D_{int} = \{D_{gb}(D_v)^{n-1}\}^{1/n}. \tag{5}$$

Diffusivity values at 600 °C are $D_{gb}=5.24\times10^{-12}$ $m^2\,s^{-1}$ (Ref. 21) and $D_v=2.00\times10^{-17}$ $m^2\,s^{-1}$ (Ref. 22). The energy ratio, $n=\gamma_{gb}/\gamma_{int}$, is calculated to be 1.41 from Eq. (3) for the tangential angle of 45°. Putting these values into Eq. (5), we get $D_{int}=1.39\times10^{-13}$ $m^2\,s^{-1}$. To the first approximation, it is found that the interface diffusivity of Cu is one order of magnitude smaller than the grain boundary diffusivity.

We can also estimate interface diffusivity using a theory proposed by Mullins *et al.*[23] They measured the depth and tangential angle of surface grooves in Cu bicrystals as a function of annealing time and calculated surface diffusivity. Careful examination of the original derivation indicated that the equations proposed by Mullins *et al.* can be used to obtain interface diffusivity simply by replacing surface terms with interface terms. According to the theory, the groove depth at annealing time, t, can be written as follows when the interface diffusion is a rate controlling process:

Downloaded 11 Jul 2008 to 130.34.135.158. Redistribution subject to AIP license or copyright; see http://jap.aip.org/jap/copyright.jsp

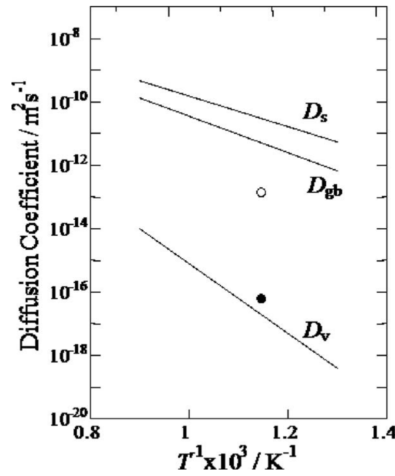

FIG. 10. Estimated interface diffusivity according to Gupta (Ref. 20, an open circle) and Mullins (Ref. 21, a solid circle) in comparison with reported diffusivity values.

$$d = 0.973(Bt)^{1/4}\tan\,\theta. \tag{6}$$

B is known as the Mullins parameter, and is given by

$$B = (\delta D_{\text{int}}\gamma_{\text{int}}\Omega)/kT. \tag{7}$$

It should be noted that the power constant of annealing time is 1/4 when interface diffusion is a rate-controlling process, whereas it is 1/3 when volume diffusion is a rate-controlling process. In the present work, the depth and the angle were measured at annealing time of 5 and 10 h. Plotting log d and log t yielded a slope of 0.276 that is in good agreement with the theoretical power constant of 1/4 in Eq. (6). Though the measured time segments are only two, the groove depth at each time segment corresponds to an average value from ten different triple points. The good agreement in the power constant suggests that the Mullins equation can be applied to the observed change of the triple-point morphology that is rate-controlled by interface diffusion. In Eqs. (6) and (7), the surface terms in the original equation by Mullins *et al.* are replaced with the interface terms of $\delta D_{\text{int}}\gamma_{\text{int}}$, with δ being interface width, D_{int} interface diffusivity, γ_{int} interface energy, and Ω atomic volume. The measured average depth of d=25.8 nm after t=10 h and the tangential angle of θ =45° yield the Mullins parameter of B=1.37 $\times 10^{-35}$ m^4 s^{-1}. In order to calculate the interface diffusivity, we use the atomic volume of Cu, $\Omega = 1.18\times 10^{-29}$ m^3; then, we have $\delta D_{\text{int}} = 6.34\times 10^{-26}$ m^3 s^{-1}. Assuming that the interface width is δ=0.5 nm, the interface diffusivity is estimated to be 6.35×10^{-17} m^2 s^{-1}.

Figure 10 compares the obtained interface diffusivity values with reported diffusivity values on surface,[24] along grain boundaries,[21] and in bulk volume.[22] The calculated values using Eq. (5) by Gupta and Eq. (7) by Mullins are indicated, respectively, by an open circle and by a solid circle. The estimated value by the Mullins model does not necessarily correspond to the interface diffusion of Cu atoms. It may correspond as well to the interface diffusion of the constituting elements in the barrier layer. The slower process between the two becomes the rate-controlling process of the morphology change at the triple points. Since the barrier layer is an oxide, the diffusion of constituting elements is likely to be much slower than the diffusion of Cu along the interface. Therefore, the estimated value by the Mullins model is considered to represent the interface diffusion of the elements in the barrier layer. On the contrary, the estimated values with two different methods are different by four orders of magnitude. The Gupta model deals with the diffusion of Cu atoms in bulk volume and considers the diffusion of the same Cu atoms along the interface that has a smaller activation energy with reference to the activation energy in bulk volume. Therefore, the estimated value by the Gupta model represents the interface diffusivity of Cu atoms.

V. SUMMARY

A thin barrier layer was self-formed by depositing a Cu-10at. %Mn alloy film on SiO_2 substrate and by subsequent heat treatment. The barrier layer maintained the diffusion barrier property at 450 °C up to 100 h and at 600 °C up to 10 h. The growth kinetics of the barrier layer was investigated by measuring the thickness of the barrier layer after heat treatment and found to follow a logarithmic rate law at 250 °C, 350 °C, and 450 °C. This logarithmic growth kinetics suggests an enhanced growth mechanism due to the presence of the electric field across the barrier layer. Detailed analysis of EELS fine-edge structure of Mn indicated the presence of ionized Mn in the Cu-Mn alloy and the presence of electric field across the barrier layer. The diffusivity at the interface between the Cu-Mn alloy and the barrier layer was also estimated by two different methods by analyzing groove formation at 600 °C. The estimated values of interface diffusivity were in reasonable agreement and found to be slower than the grain boundary diffusivity of bulk Cu.

In the application to LSI interconnect structure, the logarithmic growth kinetics is of great advantage because the barrier growth is self-limited within the range of 2 to 7 nm and is controllable by properly selecting annealing temperature and time.

ACKNOWLEDGMENTS

The work was performed under the financial support by the Japan Science and Technology Agency, Innovation Plaza Miyagi. We are grateful to Dr. H. Shibata and T. Usui at Toshiba Corporation for fruitful discussion and to Dr. M. Koide of Mitsubishi Materials Corporation for providing high-purity Cu targets.

[1] A. E. Kaloyeros and E. Eisenbraun, Annu. Rev. Mater. Sci. **30**, 363 (2000).
[2] The International Technology Roadmap for Semiconductors, Interconnect edition, (2005), p. 14.
[3] H. Kim, J. Vac. Sci. Technol. B **21**, 2231 (2003).
[4] P. J. Ding, W. A. Lanford, S. Hymes, and S. P. Murarka, J. Appl. Phys. **75**, 3627 (1994).
[5] P. J. Ding, W. A. Lanford, S. Hymes, and S. P. Murarka, Appl. Phys. Lett. **64**, 2897 (1994).
[6] M. J. Frederick and G. Ramanath, J. Appl. Phys. **95**, 3202 (2004).
[7] K. Barmak, A. Gungor, C. Cabral, Jr., and J. M. E. Harper, J. Appl. Phys. **94**, 1605 (2003).
[8] J. Koike and M. Wada, Appl. Phys. Lett. **87**, 041911 (2005).
[9] M. Haneda, J. Iijima, and J. Koike, Appl. Phys. Lett. **90**, 252107 (2007).
[10] T. Usui, H. Nasu, S. Takahashi, N. Shimizu, T. Nishikawa, M. Yoshimaru,

Downloaded 11 Jul 2008 to 130.34.135.158. Redistribution subject to AIP license or copyright; see http://jap.aip.org/jap/copyright.jsp

H. Shibata, M. Wada, and J. Koike, IEEE Trans. Electron Devices **53**, 2492 (2006).
[11]H. K. Schmid and W. Mader, Micron **37**, 426 (2006).
[12]H. Kurata and C. Colliex, Phys. Rev. B **48**, 2102 (1993).
[13]C. Wagner, Z. Phys. Chem. Abt. B **21**, 25 (1933).
[14]N. Cabrera and N. F. Mott, Rep. Prog. Phys. **13**, 163 (1948).
[15]O. Kubaschewski and B. E. Hopkins, *Oxidation of Metals and Alloys* (Butterworths, London, 1967).
[16]A. Atkinson, in *Materials Science and Technology, A Comprehensive Treatment*, Vol. 11, Structure and Properties of Ceramics, edited by M. V. Swain (VCH, Weinheim, 2006), p. 295.
[17]R. Nakatani, H. Yakame, Y. Endo, and M. Yamamoto, Jpn. J. Appl. Phys., Part 1 **42**, 3392 (2003).
[18]P. Avouris, R. Martel, T. Hertel, and R. Sandstrom, Appl. Phys. A: Mater. Sci. Process. **66**, S659 (1998).
[19]V. T. Borisov, V. M. Golikov and G. V. Sherbedinskiy, Fiz. Met. Metalloved. **17**, 881 (1964).
[20]D. Gupta, Interface Sci. **11**, 7 (2003).
[21]B. Burton and G. W. Greenwood, Met. Sci. **4**, 215 (1970).
[22]S. Fujikawa and K. Hirano, in *Proceedings of the Yamada Vth Conference on Point Defects and Defect Interactions in Metals*, edited by J. Takamura, M. Doyama, and M. Kiritani (University of Tokyo Press, Tokyo, 1982), p. 554.
[23]W. W. Mullins, J. Appl. Phys. **28**, 333 (1957).
[24]F. J. Bradshaw, R. H. Brandon, and C. Wheeler, Acta Metall. **12**, 1057 (1964).

Downloaded 11 Jul 2008 to 130.34.135.158. Redistribution subject to AIP license or copyright; see http://jap.aip.org/jap/copyright.jsp